Scour at Coastal Inlet Structures

Steven A. Hughes[1] and J. William Kamphuis[2]

Abstract: Scour at inlet navigation structures was investigated using a series of movable-bed physical models. Experiments included ebb and flood flows, sometimes combined with wave action. A new and potentially important scour mechanism was identified for situations where the ebb-flow discharge is redirected by a navigation structure. As ebb flow is deflected, flow velocities increase and a scour trench forms adjacent to the jetty.

In this paper formulations from inviscid jet theory are used to develop an easily-applied, but crude, prediction capability for maximum flow velocity in terms of entrance channel velocity and inlet geometry. A simplified scour prediction method is also provided, but much needs to be done to make it more realistic. Preliminary conclusions are given about scour produced by flood flow combined with waves.

1   Introduction

Scour hole formation adjacent to the channel-side toe and near the head of protective inlet jetty structures is a troublesome problem at many navigation inlets. Without remedial action, continued scour hole growth may result in jetty instability and partial collapse of the structure. In addition, deep scouring adjacent to the channel side of a protective jetty may be accompanied by shoaling of the maintained navigation channel, shifting the navigation channel dangerously close to the jetty.

   These inlet scour problems were investigated through a comprehensive set of movable-bed model experiments conducted jointly by Queens University in Canada and the Coastal Engineering Research Center (CERC) in the United States. The experiments examined flood-flow and ebb-flow scour that develops at inlets under various combinations of tidal flow discharge, flow direction, and incoming wave action. The goal of the experiments was to develop simple empirical relationships for

---

[1]Research Hydraulic Engineer, US Army Engineer Waterways Experiment Station, Coastal and Hydraulics Laboratory, 3909 Halls Ferry Road, Vicksburg, Mississippi 39180-6199 USA.

[2]Professor, Department of Civil Engineering, Ellis Hall, Queens University, Kingston, Ontario, K7L 3N6 CANADA.

estimating maximum scour depth in terms of easily determined parameters related to tidal discharge, channel geometry, and incident wave parameters.

From a survey of scour problems experienced at inlets (Lillycrop and Hughes 1993), it appears that one of the more important physical mechanisms causing scour at inlets during ebb flow is strong ebb currents that exit the inner bay and impinge on the structure at an angle as shown schematically by Figure 1. Laboratory observations indicated that as the ebb flow is deflected, the width of the flow parallel to the navigation structure is reduced, much like the deflection of a water jet. This results in increased flow velocity adjacent to the structure in order to maintain the same flow discharge over the reduced cross-section. Over many ebb-tidal cycles the increased velocities scour the bottom and enlarge the flow cross-sectional area until eventually flow velocities are reduced to non-scouring levels. The scour process is further complicated by the influence of short-period waves in the channel, entrainment at the flow shear interface, changes in flow velocity over the ebb cycle, and the influence of a porous jetty structure.
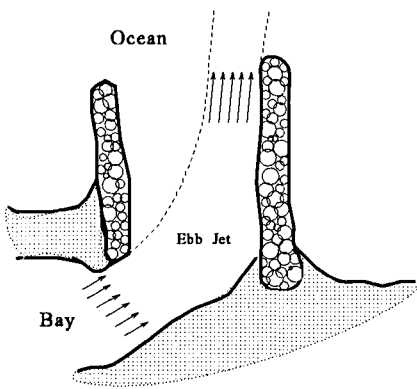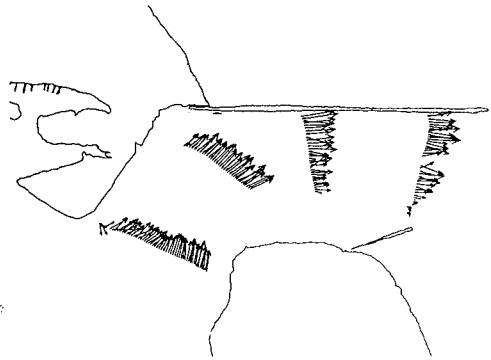
Figure 1: Ebb Flow Deflection.

Figure 2: Depth-Averaged Ebb-Flow Velocities at Ponce de Leon Inlet.

Field evidence of velocity increases due to ebb-flow deflection is shown in Figure 2, which plots depth-averaged ebb-flow velocity measurements obtained at Ponce de Leon Inlet, Florida. At the time of these measurements a scour trench had already formed adjacent to the jetty. Otherwise, the velocities would likely be even greater next to the jetty.

2   Laboratory Experiments

A series of deflected ebb-flow laboratory movable-bed model tests were conducted in a 15-m-wide wave flume at CERC with an undistorted nominal length scale of 1:20 and a water depth of 30 cm. These tests expanded on earlier studies conducted at Queens University at 1:30 scale. The experiment layout is sketched in Figure 3.

A conventional model jetty was constructed on a 45-cm-deep flat bed of fine quartz sand having mean diameter of 0.13 mm. The jetty toe was protected with a small stone scour blanket. The current manifold position and angle were adjustable to allow
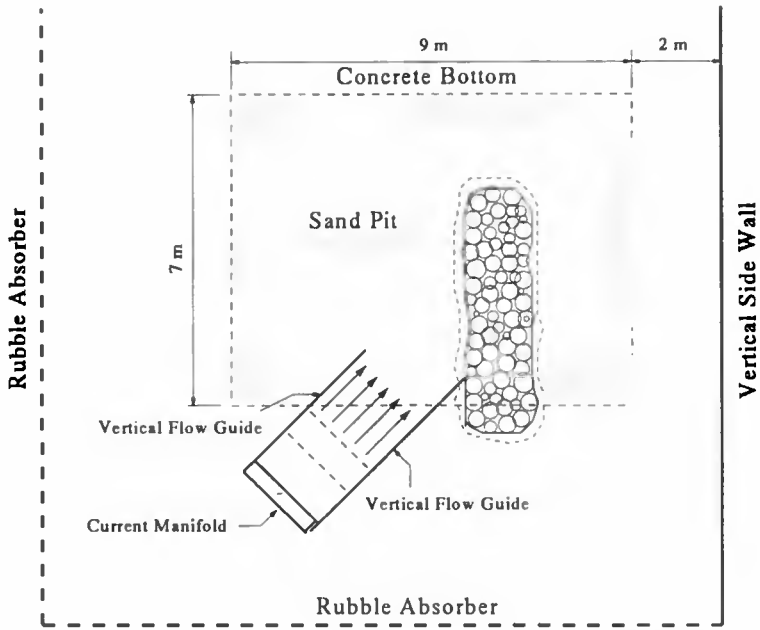
Figure 3: Ebb Flow Experiment Layout.

Figure 4: Scour After 10 Hours with 60° Deflection (View from Seaward of Jetty).

different deflection angles (30°, 45°, 60°) relative to the jetty centerline. Adjustable vertical flow guides were used to direct the ebb flow, and flow straighteners helped to make the flow more uniform before passing over the movable bed. Total flow discharge was monitored and controlled at an upstream valve.

Laboratory measurements of flow velocity throughout the study region were accomplished using an array of three SonTek acoustic Doppler current meters (ADV's) mounted on an instrument catwalk spanning the flume. At each location the ADV's recorded a 3-minute velocity time series (25-Hz sample rate) at a depth 15 cm below the water surface. (All measurement values throughout this paper are in model units.)

Mean velocity at the input entrance channel was adjusted to be slightly above the 28–30 cm/s estimated to be required for incipient motion of the sediment. Dye injection indicated the deflected flow width adjacent to the jetty narrowed considerably similar to Figure 1. This gave rise to increased velocities adjacent to the jetty and significant scour along the jetty structure. Depending on the flow deflection angle, mid-depth mean velocities adjacent to the structure varied between 40–50 cm/s at the start of the experiments while the sand bed was still horizontal and scour was in initial stages.

Experiments continued for a total of 10 hours by which time it appeared that scour had reached an equilibrium for that flow condition. A portion of the scoured sediment was transported seaward by the ebb flow and deposited in a "fan" in a deeper part of the flume, whereas some sediment was deposited in a "berm" running parallel to the scour trench. Typical scour results are illustrated by the photograph in Figure 4, which was taken from a seaward position after an experiment with a 60° deflection angle. The photograph shows that the scour apron may have helped protect the armor slope.

Post-experiment surveys of the bed were completed using a Delft bed profiler mounted on the traversing catwalk. Bed elevation data were obtained at 4-cm spacings on survey lines running perpendicular to the jetty centerline. There was 20-cm spacing between survey lines.

3 Deflected Ebb Jet Theory

3.1 Analogy to Jet Flow

The deflected ebb-flow observed in the laboratory experiments is quite similar to a two-dimensional jet impinging on a solid boundary, and an analytical approach to deflected ebb-flow hydrodynamics was developed based on this analogy. Using the notation and coordinate system detailed in Figure 5, an inviscid, potential flow solution can be specified that links the flow field to the geometry of the solid boundaries. The assumptions associated with this flow solution are given as:

- Incompressible, nonviscous, ideal fluid (no boundary layers, boundary layer separation, or flow entrainment at the jet *"free boundary"*)[1]

- Steady flow in two dimensions (horizontal bottom)

---

[1]The term *"free boundary"* refers to the interface between the jet and the adjacent still water as represented by the dashed line in Figure 1.
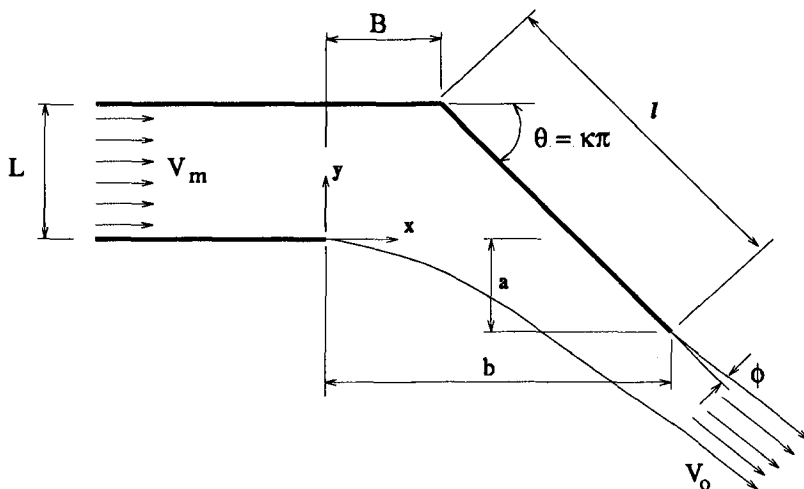
Figure 5: Ebb Jet Coordinate System.

- Nonrotational flow (velocity potential exists)

- Gravity has no effect on flow (implies relatively high velocities, and no cross-channel water surface setup due to centrifugal forces)

On solid boundaries and on flow streamlines there is the "no-flow" condition, i.e.,

$$\frac{\partial \phi}{\partial n} = 0 \tag{1}$$

and on the *"free boundaries"* pressure is assumed constant. This means that on the free boundary streamline, Bernoulli's Equation is given as

$$\frac{V_o^2}{2} + gz = constant \tag{2}$$

Neglecting gravitational effects reduces the free-boundary condition of Eqn. (2) to

$$V_o = Constant \tag{3}$$

3.2 Potential Flow Solution

The solution to this particular jet-flow problem was given in Gurevich (1965). Without presenting details, the solution was found by conformally mapping the jet and its boundaries into a unit circle in the complex plane. Conformal mapping is a typical approach for this family of jet-flow problems. Other techniques are unsuccessful because the location of the jet free boundaries is not known *a priori*.

The resulting solution[2] is expressed as the following three equations (Eqns. 4–6)

---

[2]Note that in Gurevich (1965), page 63, the denominator of the second term under the integral of Eqn. (6) was incorrectly given as "$t + (1/h)$" rather than the correct value of "$t - (1/h)$".

$$\frac{\ell}{L} = \frac{h^\kappa}{\pi} \int_0^1 \frac{d\xi}{\xi^\kappa} \left[\frac{1}{\xi + h} + \frac{1}{\xi + (1/h)} - \frac{2[\xi + \cos(\beta)]}{\xi^2 + 2\xi \cos(\beta) + 1} \right] \tag{4}$$

$$\frac{a}{L} = 1 - \frac{\ell}{L} \sin(\pi\kappa) \tag{5}$$

$$\frac{b}{L} = \frac{\ell}{L} \cos(\pi\kappa) - \frac{h^\kappa}{\pi} \text{V.P.} \int_0^1 \frac{dt}{t^\kappa} \left[\frac{1}{t - h} + \frac{1}{t - (1/h)} - \frac{2[t - \cos(\beta)]}{t^2 - 2t \cos(\beta) + 1} \right] \tag{6}$$

where "V.P." in Eqn. (6) means take the Cauchy principal value of the integral. In these equations, the parameter h is defined by the expression

$$h^\kappa = \frac{V_m}{V_o} \tag{7}$$

and the angle β is related to the jet exit angle, ϕ, by the geometric relationship

$$\beta = \frac{\phi}{\kappa} + \pi \tag{8}$$

with both angles given in radians.

The main difficulty with this solution is that the equations explicitly solve for the deflected jet geometry (ℓ/L, a/L, b/L) given the entrance and exit velocities (V_m, V_o), jet deflection angle ($\theta = \kappa\pi$), and jet exit angle (ϕ). In application to inlets, the geometry is usually known, and the flow solution is sought. Because the equations cannot be inverted, the only recourse is an iterative or nomogram solution.

Figure 6 presents an example of a nomogram that was generated for an ebb-flow deflection angle of 45° ($\kappa\pi = \pi/4$). This nomogram was constructed by solving Eqns. (4) and (6) at over 850 evenly distributed grid points bounded by the axes shown in Figure 6, and then contouring the results. The solid lines are contours of equal values for ℓ/L and the dashed lines represent constant values of b/L. For a given inlet geometry the unique solution is found at the intersection of the appropriate values of ℓ/L and b/L. The jet exit angle, ϕ, in degrees is read from the abscissa, and the velocity function, h, is read from the ordinate. The unknown velocity, V_o, corresponding to a value of V_m can now be determined from Eqn. (7). Figure 7 illustrates the variation in velocity ratio, V_o/V_m as a function of ebb-jet deflection angle, θ, and geometry parameter, B/L (see Figure 5 for definition of B).

Once values of h and ϕ are known, it is also possible to specify the location of the inviscid "free boundary" using the following equations that were derived based on Gurevich's (1965) formulation of the complex velocity potential.

$$dx = \frac{Lh^\kappa}{\pi} \left[\frac{\sin \sigma\kappa + h \sin \sigma(1 - \kappa)}{(\cos \sigma - h)^2 + \sin^2 \sigma} + \frac{\sin \sigma\kappa + \frac{1}{h} \sin \sigma(1 - \kappa)}{(\cos \sigma - \frac{1}{h})^2 + \sin^2 \sigma} - \right. \tag{9}$$

$$\left. - \frac{\sin \sigma\kappa + \sin [\sigma(1 - \kappa) - \beta]}{2 - 2\cos(\sigma - \beta)} - \frac{\sin \sigma\kappa + \sin [\sigma(1 - \kappa) + \beta]}{2 - 2\cos(\sigma + \beta)} \right] d\sigma$$
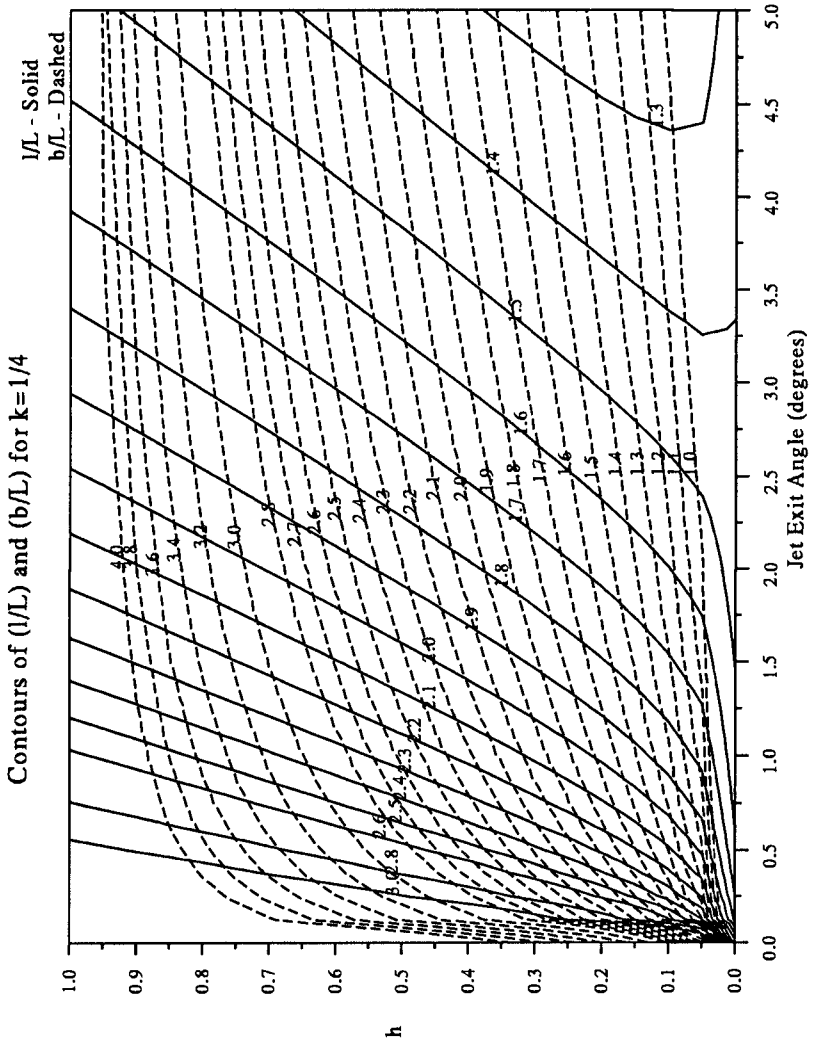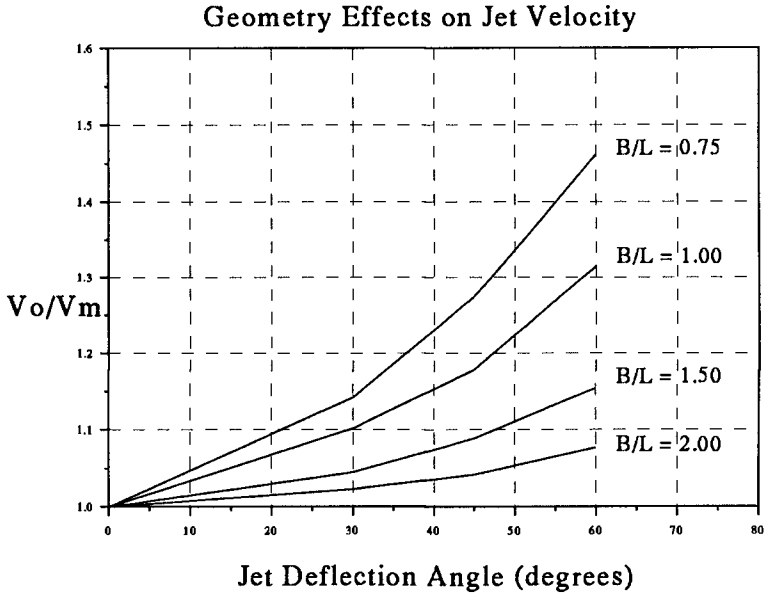
Figure 6: Nomogram for Ebb-Flow Deflection Angle of 45°.

Geometry Effects on Jet Velocity

Figure 7: Effect of Geometry on Ebb Jet Velocity Ratio.

$$dy = \frac{Lh^\kappa}{\pi}\left[\frac{\cos\sigma\kappa - h\cos\sigma(1-\kappa)}{(\cos\sigma - h)^2 + \sin^2\sigma} + \frac{\cos\sigma\kappa - \frac{1}{h}\cos\sigma(1-\kappa)}{(\cos\sigma - \frac{1}{h})^2 + \sin^2\sigma} - \right.$$
$$\left. - \frac{\cos\sigma\kappa - \cos[\sigma(1-\kappa) - \beta]}{2 - 2\cos(\sigma - \beta)} - \frac{\cos\sigma\kappa - \cos[\sigma(1-\kappa) + \beta]}{2 - 2\cos(\sigma + \beta)}\right]d\sigma \qquad (10)$$

Values of x, y on the free boundary relative to the origin shown in Figure 5 are found by numerically integrating Eqns. (9-10) between zero and different values of σ lying between $0 \longrightarrow \beta$, where β (in radians) is given by Eqn. (8).

3.3   Caveats!

It is important to note that the inviscid jet theory does **NOT** include any allowance for the following important *"real world"* effects related to deflected ebb flow at inlets:

- Turbulent flow entrainment between the ebb jet and adjacent still water

- Boundary layer losses due to the jetty structure and the bottom

- Effects of gravity on the ebb flow (possible secondary flows)

- Sloping, porous rubble-mound structures rather that vertical side walls

- Nonuniform entrance flow distribution

- Nonuniform depth in approach channel

- Wave effects on the ebb jet

Nevertheless, this initial flow approximation technique provides a conservative estimate of maximum flow velocity that would occur in the absence of the "real world" effects, and it can be used as a foundation on which to incorporate empirical approximations for these effects.

4   Comparison to Measurements

Figure 8 plots time-averaged velocity vectors measured at mid-depth for an experiment where the entrance channel was oriented 60° to the jetty. The average entrance velocity was $V_m = 32$ cm/s, and the dashed line in the figure is the inviscid *"free boundary"* calculated using Eqns. (9) and (10) with appropriate values of h and ϕ from the nomograms. Velocity increase along the jetty is clearly evident, as is flow entrainment along the ebb jet free boundary.

Ebb-jet theory estimates of maximum velocity, V_o, are compared to measured values near the seaward end of the jetty in Figure 9. Flow deflection angles of 60° (upper) and 45° (lower) are shown, and the plots are oriented with the structure to the left side (view from offshore). The theory predicts a constant velocity from the jetty out to the jet free boundary, at which point the velocity becomes zero at the interface.

Close to the jetty, the inviscid jet theory provides good estimates based only on geometry and entrance velocity, V_m (32 cm/s). Further away from the structure, flow entrainment between the ebb jet and adjacent still water had a significant impact.

Neglected altogether is the possibility that some of the flow acceleration might be due to secondary flows generated by a slope in the water elevation caused by centrifugal forces as the flow is deflected. This mechanism is thought to be important in river bends. Field measurements at an inlet where ebb flows are deflected by a structure would provide insight into whether secondary flows may also be an important factor in flow acceleration and subsequent scour.

5   Conservative Scour Prediction

Inviscid jet theory, coupled with flow continuity, can provide very crude (and overly conservative) scour estimates for deflected ebb-jet flows. Flow continuity requires the discharge at the entrance section (Q_m) be equal to the discharge at the narrowest part of the jet (Q_o), i.e.,

$$V_m \, d_m \, L = V_o \, d_o \, W_o \quad \text{or} \quad \frac{V_m}{V_o} = \frac{d_o}{d_m} \frac{W_o}{L} \qquad (11)$$

where d_m and d_o are the total depths at the entrance and narrow section, respectively, and W_o is the width of the jet at its narrowest. Assuming an initially flat bottom where $d_m = d_o$, the width ratio W_o/L in Eqn. (11) can be expressed as
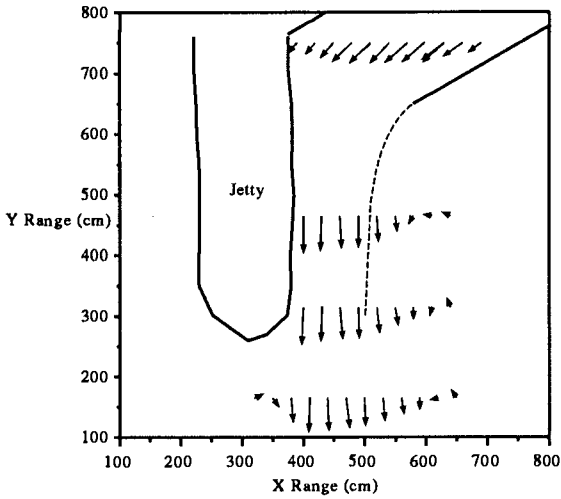
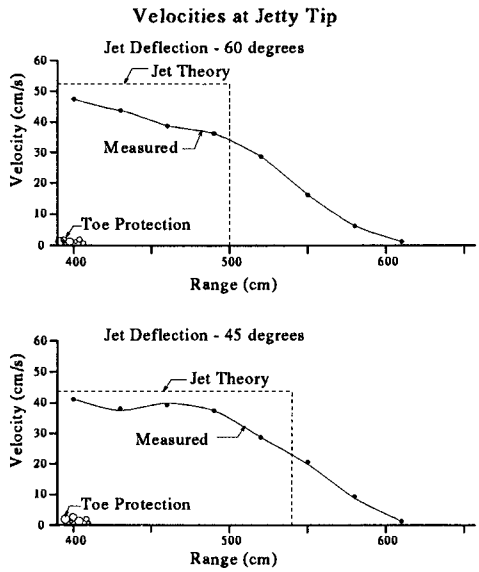Figure 8: Measured Mid-Depth Velocities for 60° Deflection Angle.

Figure 9: Ebb-Jet Theory Compared to Mid-Depth Velocity Measurements.

$$\frac{W_o}{L} = h^\kappa \tag{12}$$

where the velocity ratio was replaced by Eqn. (7). If we assume the velocity, V_m, in the entrance channel is just at the sediment incipient motion criteria, we expect the bottom to erode at the narrowest part of the ebb jet until the velocity at that location reduces from V_o to V_m. Provided the width of the jet does not change, the depth increase necessary to maintain flow discharge is found from Eqn. (11) with $V_o = V_m$ and W_o/L given by Eqn. (12), i.e.,

$$\frac{d_o}{d_m} = h^{-\kappa} \tag{13}$$

Figure 10 shows two applications of this simplified scour prediction method compared to movable-bed model scour results. The dashed line indicates scour prediction using inviscid jet theory. Obviously, neglecting the effects of shear flow entrainment and bottom boundary layer flow reduction (and possibly secondary flows) has resulted in substantial over-prediction of scour. The assumption of constant W_o is also suspect.

6   Flood Scour Observations

Kidney-shaped scour holes situated at the tips of coastal inlet structures are a commonly observed type of scour. In some instances these scour holes are permanent features, but don't appear to threaten the structure toe. In other cases, structure toe instability has resulted with subsequent unraveling of the head armor layer and structure damage.

Preliminary tests conducted at Queens University examined development of scour holes at jetty heads under various combinations of flood-flow magnitude and direction, wave severity, and incident wave directions of -20°, 0°, and $+30^o$ relative to the jetty axis. In these tests the most severe jetty-tip scouring under flood flow currents occurred when both waves and currents approached from a -20° direction as illustrated in Figure 11.

Apparently, flood flow is accelerated as it is bent around the jetty tip similar to the classical case of potential flow around a sharp corner. The addition of waves from the same direction as the current resulted in wave diffraction around the jetty tip, which when combined with the current, increased the depth and areal extent of the scour.

7   Conclusions

Based on movable-bed laboratory experiments, a new and potentially important scour mechanism has been identified for situations where the ebb-flow discharge is redirected by an inlet navigation structure. As the ebb flow is deflected, flow velocities increase resulting in the formation of a scour trench adjacent to the jetty structure toe. This flow situation was recognized to be somewhat analogous to a free jet impinging on a wall, and inviscid jet theory was used to develop an easily-applied, but crude, prediction capability for maximum velocity in terms of entrance channel velocity and
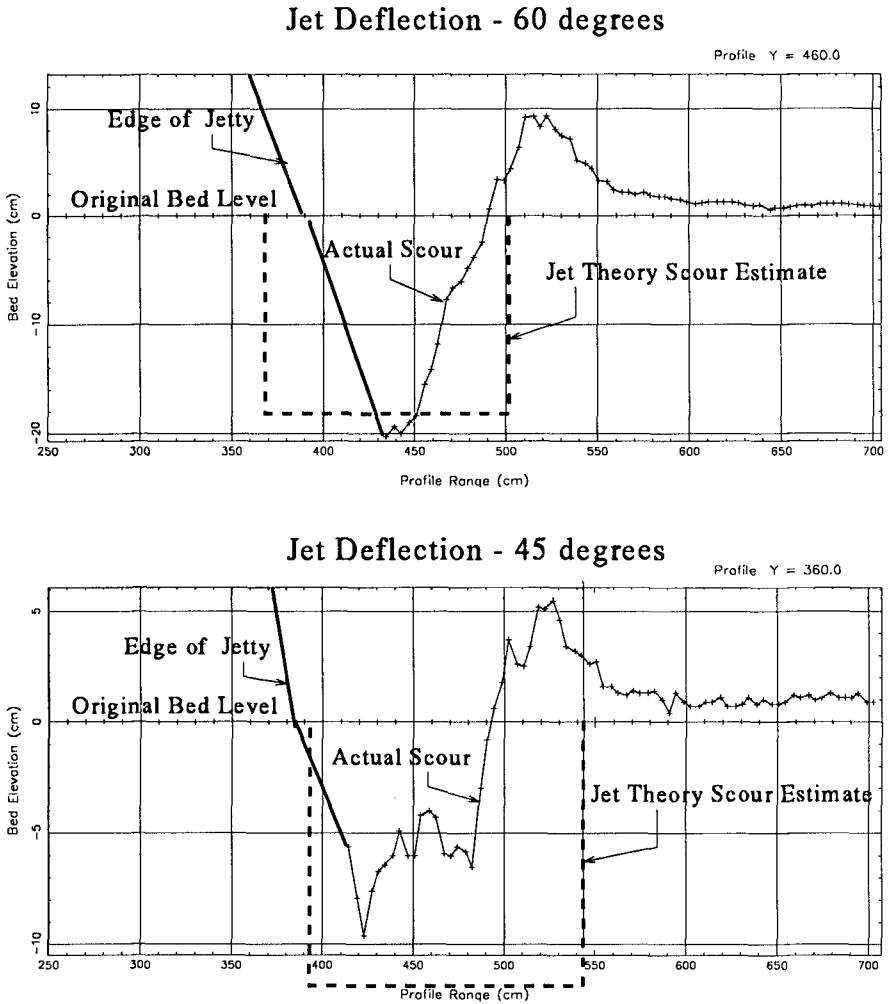
Jet Deflection - 60 degrees

Profile Y = 460.0

Edge of Jetty

Original Bed Level

Actual Scour

Jet Theory Scour Estimate

Bed Elevation (cm)

Profile Range (cm)

Jet Deflection - 45 degrees

Profile Y = 360.0

Edge of Jetty

Original Bed Level

Actual Scour

Jet Theory Scour Estimate

Bed Elevation (cm)

Profile Range (cm)

Figure 10: Conservative Scour Estimates for Two Experiments.
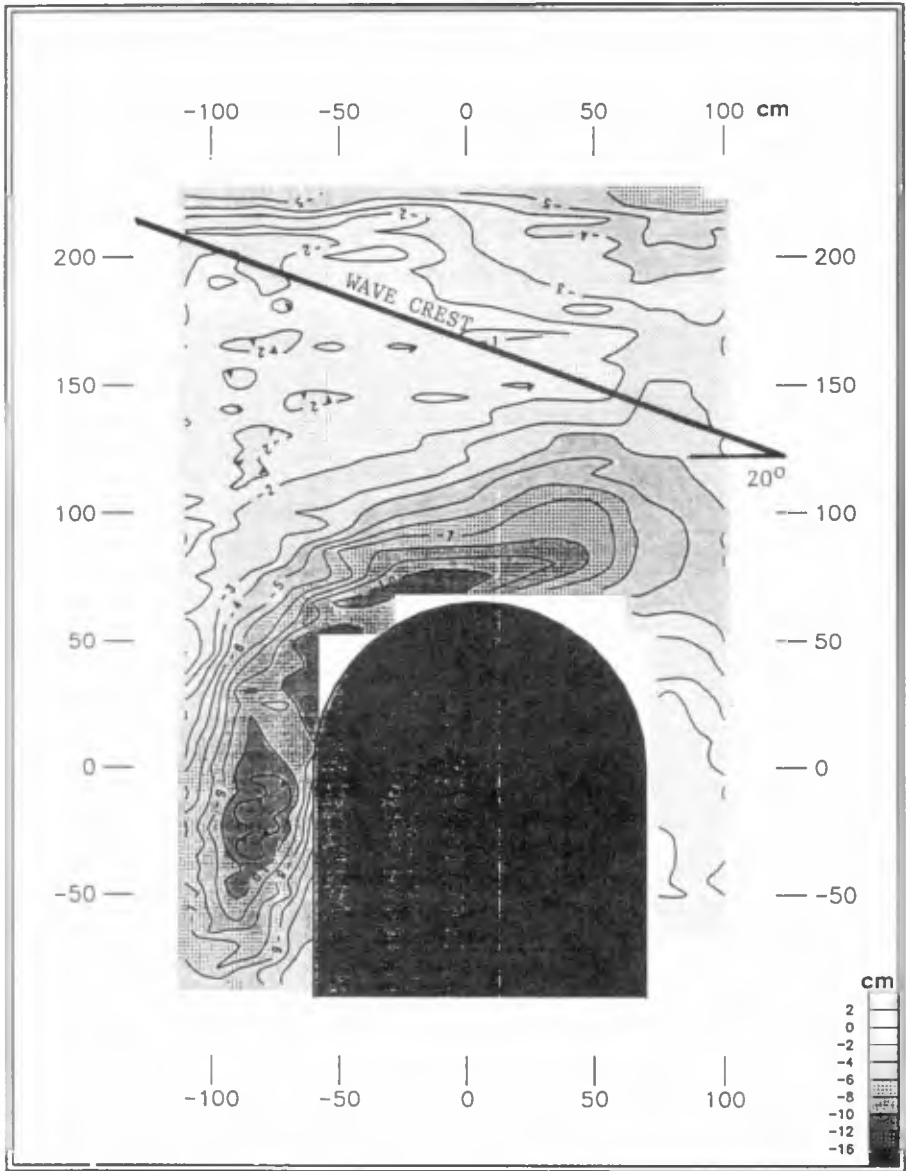
Figure 11: Example of Flood-Flow Scour Model Results.

boundary geometry. Comparison of inviscid theory to laboratory measurements indicated reasonable agreement near the jetty structure, but over-prediction away from the structure due to flow entrainment at the shear interface between the ebb-jet and adjacent still water.

A simple, overly conservative, scour prediction method was offered based on inviscid jet theory, but the method suffers from not including empirical adjustments for the "real world" effects of shear flow entrainment and bottom boundary layers. However, this inviscid theory could be used as a starting point for incorporating these necessary features. Future efforts will extend and refine these preliminary design tools.

An initial examination of movable-bed model experiments simulating scour holes produced near the tips of jetties by flood currents indicated that the most severe erosion occurs on the lee side of the jetty tip when currents and waves approach at an angle to the jetty centerline. Although currents alone are sufficient to create scour holes, the addition of waves promotes more rapid scour to greater depths over a wider area.

8 Acknowledgements

9 References

Gurevich, M. I. (1965). *Theory of Jets in Ideal Fluids*, Translated from the Russian by R. L. Street and K. Zagustin, Academic Press, New York.

Lillycrop, W. J., and Hughes, S. A. (1993). "Scour Hole Problems Experienced by the Corps of Engineers; Data Presentation and Summary," Miscellaneous Paper CERC-93-2, US Army Engineer Waterways Experiment Station, Coastal Engineering Research Center, Vicksburg, Mississippi.